African easterly waves in 30-day high-resolution global simulations: A case study during the 2006 NAMMA period

Bo-Wen Shen,[1,2] Wei-Kuo Tao,[2] and Man-Li C. Wu[2]

Received 15 June 2010; revised 23 July 2010; accepted 4 August 2010; published 18 September 2010.

[1] In this study, extended-range (30-day) high-resolution simulations with the NASA global mesoscale model are conducted to simulate the initiation and propagation of six consecutive African easterly waves (AEWs) from late August to September 2006 and their association with hurricane formation. It is shown that the statistical characteristics of individual AEWs are realistically simulated with larger errors in the 5th and 6th AEWs. Remarkable simulations of a mean African easterly jet (AEJ) are also obtained. Nine additional 30-day experiments suggest that although land surface processes might contribute to the predictability of the AEJ and AEWs, the initiation and detailed evolution of AEWs still depend on the accurate representation of dynamic and land surface initial conditions and their time-varying nonlinear interactions. Of interest is the potential to extend the lead time for predicting hurricane formation (e.g., a lead time of up to 22 days) as the 4th AEW is realistically simulated. **Citation:** Shen, B.-W., W.-K. Tao, and M.-L. C. Wu (2010), African easterly waves in 30-day high-resolution global simulations: A case study during the 2006 NAMMA period, *Geophys. Res. Lett.*, *37*, L18803, doi:10.1029/2010GL044355.

1. Introduction

[2] Extending the lead time in the prediction of hurricanes is important for saving lives and reducing damage but is very difficult to achieve with numerical models. Though global models have been used to study hurricane climate, further improvements in simulating the exact timing and location of hurricanes is still desired. Recent advances in high-resolution global models and supercomputing technology have shown the potential to achieve this. A key question to be answered is: under what conditions can the lead time for the prediction of a mesoscale hurricane be extended?

[3] It has been suggested that hurricane activity can be modulated by large-scale flows such as AEWs, which implies that the accurate simulation of AEWs may make it possible to improve the prediction of hurricane formation. Being characterized by an average westward-propagation speed of 11.6 m/s, an average wavelength of 2000~4000km, and a period of about 2 to 5 days, AEWs appear as one of the dominant synoptic weather systems in West Africa during the summertime (from June to early October). Previous studies showed that some AEWs could develop into hurricanes in the Atlantic and even East Pacific regions [e.g., *Carlson*, 1969] and that nearly 85% of intense hurricanes have their origins as AEWs [e.g., *Landsea*, 1993].

[4] The initiation of an AEW is found to be related to the release of barotropic and/or baroclinic instability associated with an African easterly jet (AEJ), and the maintenance of the AEJ could be replenished by diabatically-forced meridional circulations associated with the Saharan heat low region and ITCZ [*Thorncroft and Blackburn*, 1999]. More recent studies [*Hall et al.*, 2006; *Thorncroft et al.*, 2008] have indicated the importance of finite amplitude initial perturbations (e.g., a strong convective event) in triggering the genesis of AEWs. While AEWs could modulate the features of the Inter-Tropical Discontinuity (ITD), where the African northeasterly trade winds and southwesterly monsoon flows meet [e.g., *Berry and Thorncroft*, 2005, and references therein; *Wu et al.*, 2009], the diabatic heating associated with the ITD over the African continent may further amplify AEWs. To this end, recent studies suggest AEWs and the AEJ should be viewed as an integrated system in order to improve the understanding of their interaction with surface processes and diabatic convection [e.g., *Cornforth et al.*, 2009]. In deference to this view, to extend the lead time for predicting hurricanes that originate near the Cape Verde islands, it is important to accurately simulate the multiscale interactions between hurricanes, AEWs, and the AEJ as well as the impacts of surface mechanics and thermal processes on the simulations of these multi-scale systems, as illustrated in Figure S1 of the auxiliary material.[1]

[5] The NASA African Monsoon Multidisciplinary Analyses (NAMMA) field campaign was launched in August 2006, providing a great opportunity to characterize the frequency of AEWs, their evolution over continental western Africa. During the 30-day observation period between late August and late September, there were six AEWs documented that appeared over Africa, propagated westward, and then passed by the Cape Verde Islands. In early September, an observed AEW developed into a Cape Verde storm–Hurricane Helene [*Brown*, 2006]. In this study, NAMMA observations and NCEP analyses are used to examine the multiscale interactions of simulated AEWs, with the aim of addressing the question of whether and how consecutive initiation of multiple AEWs can be improved. The long-term goal is to extend the previous study by *Shen et al.*, 2010, who examined the role of hierarchical multiscale interaction on the formation of Nargis (2008), to understand the extent to which large-scale AEWs could determine the timing and location of tropical cyclone (TC) genesis. This begins with examining the potential predictability of AEW

[1]ESSIC, UMCP, College Park, Maryland, USA.
[2]NASA Goddard Space Flight Center, Greenbelt, Maryland, USA.

[1]Auxiliary materials are available in the HTML. doi:10.1029/2010GL044355.

Table 1. Sensitivity Experiments for Examining the Dependence of AEW Simulations on Different Dynamic ICs, Land Surface ICs, SSTs and Modified Guinea Highlands (Reduced Height)[a]

Exp ID	Dynamic IC	Land Surface IC	SST	Guinea Highlands	Remarks
cntl	08/22	08/22	w		
A	08/23	08/23	w		
B	08/24	08/24	w		
C	08/25	08/25	w		
D	08/22	Cold-start	w		
E	08/22	06/22	w		
F	08/22	08/22	c		
G	04/22	08/22	w		date changed to be 08/22/2006
H	06/22	08/22	w		date changed to be 08/22/2006
I	08/22	08/22	w	Heights scaled by factor of 0.6	

[a]w (or c) indicates weekly (or climate).

initiation and evolution and their association with hurricane formation (e.g., Helene) with a high-resolution global model.

2. Model and Numerical Approach

[6] The global mesoscale model is composed of three major components: 1) finite-volume dynamics, 2) NCAR CCM3 physics, and 3) the NCAR Community Land model [*Lin*, 2004; *Atlas et al.*, 2005; *Shen et al.*, 2006]. In this study, the 0.25° model with a large-scale condensation scheme [e.g., *Shen et al.*, 2010] is used for performing experiments. Dynamic initial conditions (ICs) and sea surface temperatures (SSTs) are derived from Global Forecast System (GFS) T384 (~ 35km) analysis data and 1° optimum interpolation SSTs from the National Centers for Environmental Prediction (NCEP). In previous studies by other researchers, the soil moisture [e.g., *Hsieh and Cook*, 2005] or meridional surface temperature gradient [*Cornforth et al.*, 2009] is prescribed. To generate land surface (and physics) ICs that are consistent with the dynamic ICs, warm-start runs of at least two years were performed. To examine the sensitivity of AEW simulations to different parameters, 9 additional experiments were conducted (1) by initializing the model with three different dynamic ICs at 0000 UTC for three consecutive days (Exps. A, B, and C), (2) by applying different land surface ICs (used by the land model; Exps. D and E), or replacing weekly SSTs with climatological SSTs (Exp F), and (3) by using a dynamic IC in a different month (Exps. G and H), and (4) by reducing the height of the Guinea Highlands (Exp. I). Table 1 gives a summary of these experiments. The procedure for detecting AEWs and the formation of a TC is discussed by *Sander and Jones* [2008] and by *Shen et al.* [2010], respectively. Figures S1–S8 are included in the auxiliary material to provide additional support.

3. Numerical Results

[7] In the following section, the 30-day control run initialized at 0000 UTC August 22, 2006 is first verified against the NCEP analysis before discussing the sensitivity experiments. The modulation of Helene's formation by one of the AEWs is discussed for the control run.

3.1. AEWs and AEJ in the 30-Day Control Run

[8] Figure 1 shows NCEP analyses (Figure 1, top) and 0.25° simulations (Figure 1, bottom) during the period August 22 to September 21, 2006. Time-longitude diagrams of 850-hPa meridional winds averaged over 5° to 20°N are shown in Figures 1a and 1d. During this 30-day period, both the model simulations and analysis indicate the occurrence of six westward propagating AEWs. These waves have a timescale of 3–5 days, a wavelength of about 2000–2500 km, and a propagation speed of about 10 m/s. Overall, the model simulations are in good agreement with the analysis, especially over the Africa continent. Spatial and temporal variations exist but are within one characteristic (time and spatial) scale. The strong wind shear along 20°W during 11–13 September, as shown by the black circle in Figure 1d, roughly indicates the formation of Hurricane Helene.

[9] Figures 1b and 1e display altitude-latitude cross sections of zonal winds averaged over the 30-day period along longitude 10°E from the control run and analysis, respectively. Both show a low-level jet with a maximum of around 10–14 m/s at (14°N, 600 hPa), which is called the AEJ [*Thorncroft and Blackburn*, 1999]. At about 200 hPa and equatorward of the AEJ, the model simulates an upper-level tropical easterly jet (TEJ), which appears at the right height but has a stronger intensity between 9°N and 15°N. Below and south of the AEJ, a low-level westerly monsoon flow is simulated (Figure 1e) in good agreement with the NCEP analysis (Figure 1b). Figures 1c and 1f show the same fields but along longitude 20°E. Overall, the model simulation is in good agreement with the NCEP analysis, but the simulated AEJ is slightly weaker.

[10] Figure 2a (Figure 2b) shows the spatial distribution of 600-hPa zonal winds (850-hPa temperatures) averaged over the entire 30 days for the NCEP analysis; Figure 2c (Figure 2d) shows the corresponding model simulations. Overall, the winds and temperatures are simulated realistically with respect to the analysis. The simulated 600-hPa AEJ along latitude 15°N, however, is weaker (e.g., in the area of 10°W-5°E and 15°–25°N) and doesn't extend to the west and north as far as the corresponding one in the analysis. The AEJ could be maintained or replenished by the diabatically-driven meridional circulation, which depends on the distribution of the surface temperature. Thus, as shown in Figures 2b and 2d (and the correlation coefficients in Figure S2), good agreement between the simulated 850-hPa temperatures and the analysis provides a good opportunity to verify the role of the meridional circulation in the evolution of the AEJ, which is the subject of further study.

3.2. Sensitivity Experiments

[11] Time-longitude cross sections of meridional winds averaged over latitudes 5°N–20°N for each of the 9

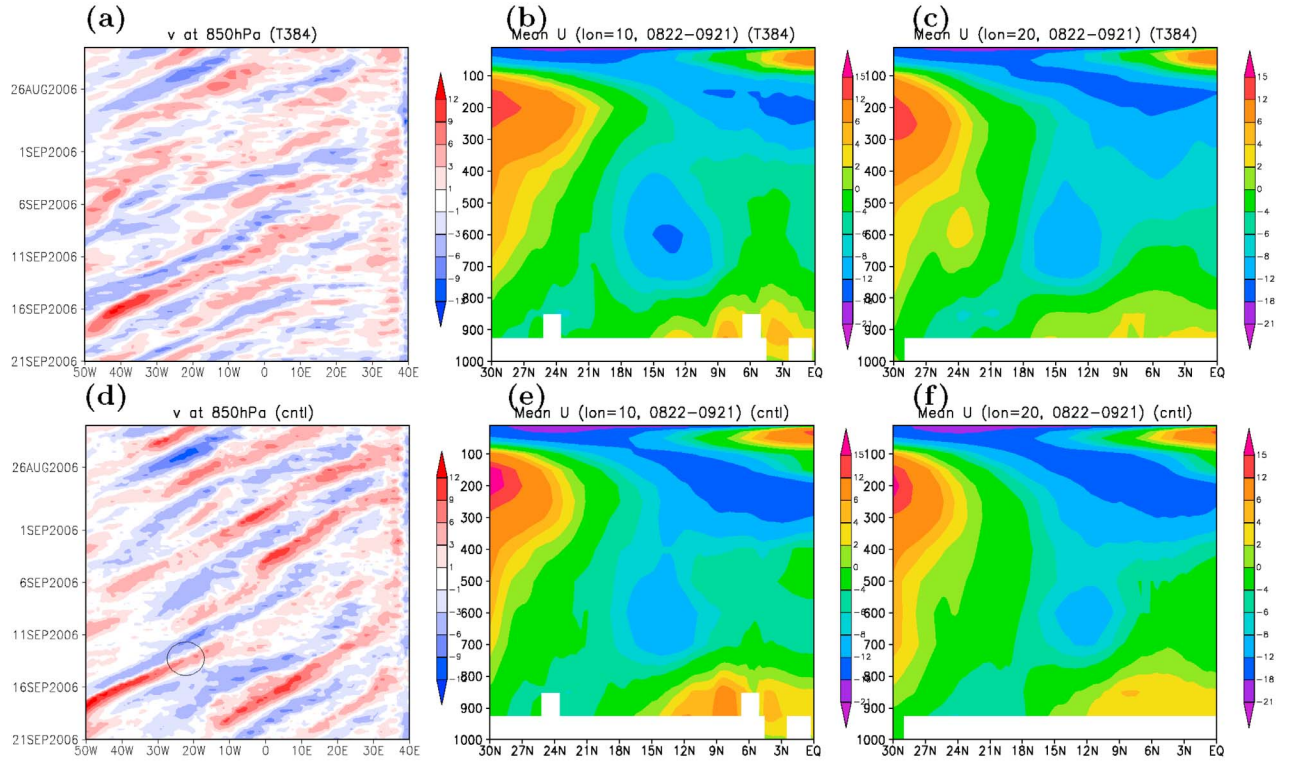

Figure 1. Six AEWs and an AEJ from (top) GFS analysis and (bottom) a 30-day simulation initialized at 0000 UTC August 22, 2006. (a, d) Time-longitude diagrams of meridional winds averaged over latitudes 5–20°N from 22 August to 21 September, 2006. Height-latitude cross sections of time-averaged zonal winds along longitude (b, e) 10°E and (c, f) 20°E, respectively. The black circle roughly indicates the timing and location of Helene's formation.

experiments are shown in Figures 3a–3i, respectively. Figures 3a–3c show the simulations initialized at 0000 UTC from 23–25 Aug. As the characteristic time scale of AEWs is about 3–5 days, the period 23–25 Aug spans a different phase of the initial (the 1st) AEW. Overall, initiation and propagation of the AEWs in the three experiments are simulated comparably, though variations exist within one characteristic scale. However, a systematic study to under-

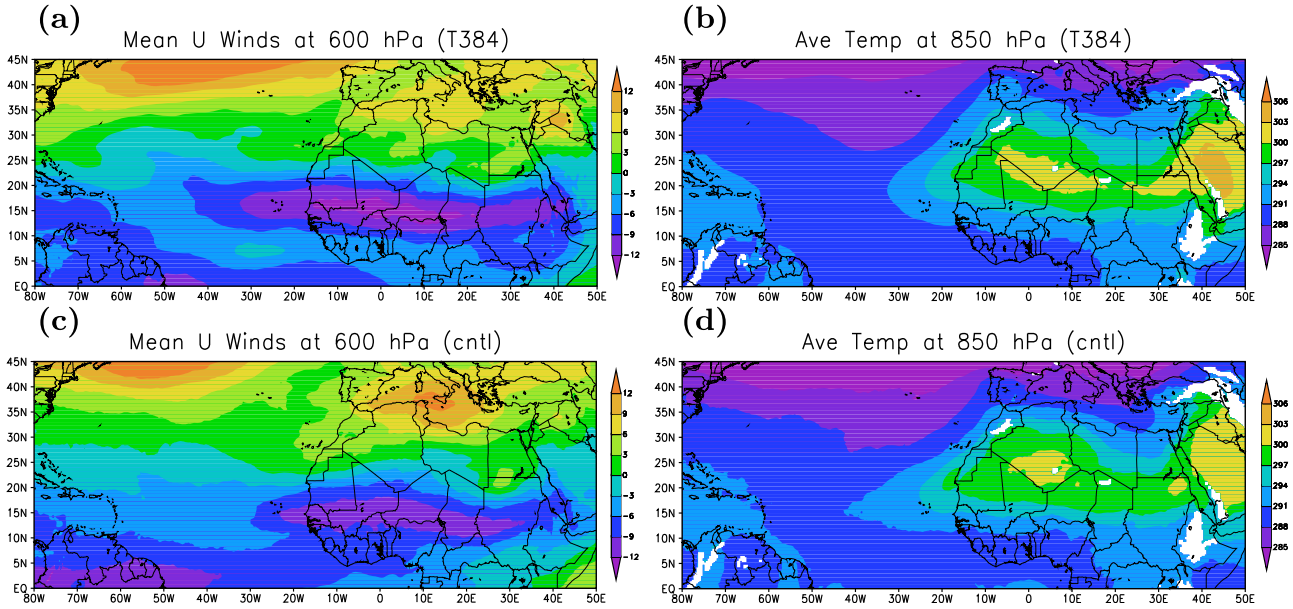

Figure 2. Thirty-day averaged fields from (top) GFS analysis and (bottom) model simulations. (a, c) Average zonal winds (m/s) at 600 hPa and (b, d) average temperatures (°C) at 850 hPa.

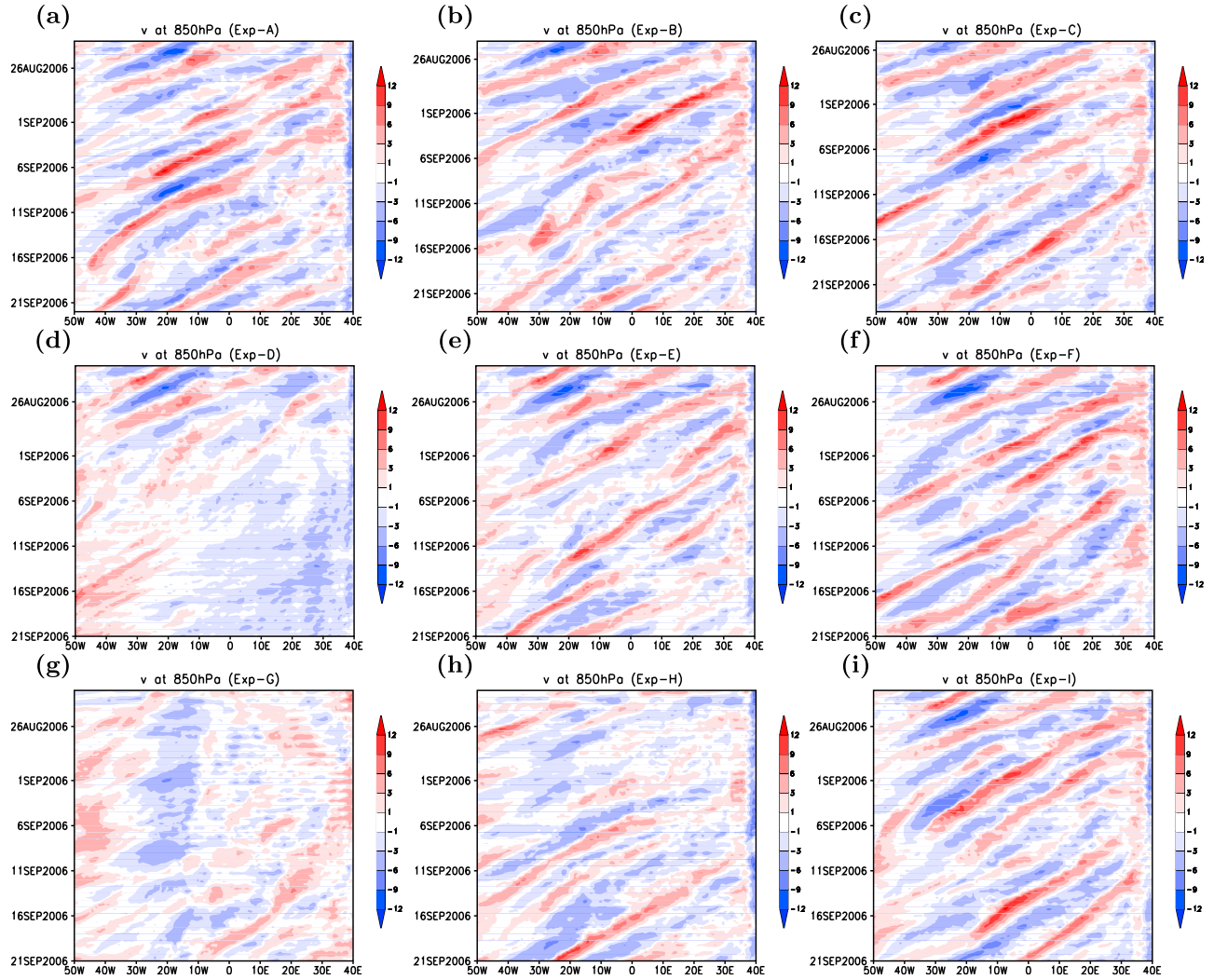

Figure 3. Sensitivity of AEW simulations to different dynamic ICs, land surface ICs, different SSTs, and the height of Guinea Highland (reduced). (a–i) Simulated meridional winds from Exps A–I.

stand the impact of the different ICs (e.g., the phase difference in the initial AEW) on the successive initiation of AEWs and their modulation on hurricane formation is still desired but beyond the scope of this study.

[12] Land surface processes may be important for the maintenance of the AEJ and thus for the initiation of AEWs. Figure 3d shows model results initialized with the same dynamic and physics ICs but with land surface ICs from a cold start run. This run simulates the evolution of the initial AEW with satisfaction up to 8–9 days but fails to simulate the initiation of any "realistic" AEWs. As shown in the Figure S5, the initial AEJ dissipates quickly during the first 3–5 days of simulation. In comparison, Exp E (Figure 3e), which uses land surface ICs derived from a previous run on 22 June, can realistically capture the initiation of AEWs over land. However, larger (timing) errors appear in the 4th, 5th, and 6th AEWs, and weaker downstream development over the ocean (e.g., for the 4th AEW) is observed. In comparison with the land surface processes, oceanic processes in the simulations of AEWs are investigated with a simple experiment by replacing the weekly SSTs with climatological SSTs. This run (Figure 3f) shows that the evolution of the first four AEWs is comparable to those in the control run. Differences appear in the 5th and 6th AEWs and shows that the effects of using climatological SSTs on the simulation of AEW initiation begin to occur after 15–20 days of integration, assuming that the synoptic-scale environmental flows were first changed and then impacted the initiation of AEWs.

[13] The next two experiments are designed to examine the impact of different dynamic ICs from different months. With the same physics and land surface ICs, Exps G and H are performed using the dynamic ICs from 22 April and June, respectively; the timestamps are changed to 22 Aug in order to keep the same model physics (e.g., radiation) and land model configurations as the control run. In Exp G (Figure 3g), no realistic AEW signals are simulated during the first 20 days of simulation, and later a less accurate AEW appears and propagates westward. Consistently, an AEJ gradually develops after 20–25 days of integration (Figure S5). In comparison, Exp H is able to simulate multiple AEW signals with some degree of satisfaction. However, large discrepancies in timing and location exist.

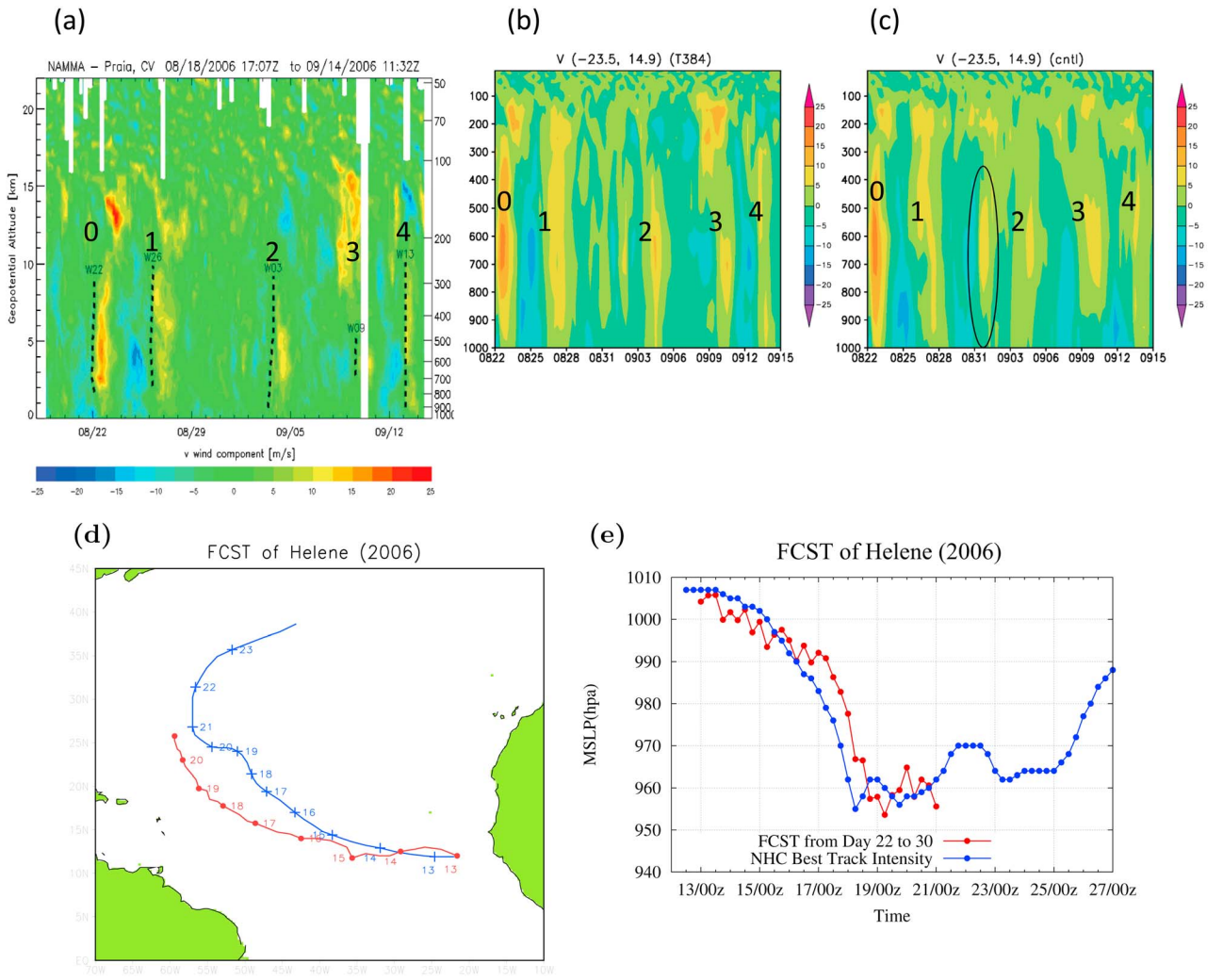

Figure 4. Time-altitude cross sections of meridional winds at (23.5°W, 14.9 ° N) from (a) NAMMA observations [*Schmidlin et al.*, 2007], (b) GFS analysis and (c) model simulation. (d) Track and (e) intensity forecasts for Hurricane Helene from Day 22 to 30. Red and blue lines indicate model predictions and best tracks, respectively.

[14] The last experiment is used to examine the mechanical effects of the Guinea Highlands on the AEW simulations (e.g., the 4th AEW) by multiplying the mountain heights by a factor of 0.6, which can mimic the effect of less accurate mountain heights in a coarse-resolution model. Figure 3i shows that the initiation of the 4th, 5th and 6th AEWs are influenced by this change, and the downstream development of AEWs (e.g., the 2nd and 4th AEWs) becomes weaker.

[15] Our sensitivity experiments, though still preliminary, show that accurate representations of land surface processes are crucial for improving the simulations of the AEWs and AEJ. Thus, in a future study, the impact of land surface processes on the evolution of an AEJ will be investigated and thus the impact of an AEJ on the simulation of AEW initiation.

3.3. Modulation on Hurricane Genesis

[16] Time-altitude cross sections of meridional winds at (23.5°W, 14.9°N) are shown in Figures 4a–4c for NAMMA observations, NCEP analysis and model results from the control run, respectively. Both the NCEP analysis and model results are averaged over a 2° box. In general, the timing and location of the simulated maximum southerly winds (indicated by a yellow color) are quite close to those from the NAMMA observations and NCEP analysis except that an additional signal appears on about 31 Aug. This event, which can be also identified by *Zipser et al.* [2009, Figure 2b], is stronger than the one in the NCEP analysis and has a time lag of about 1 day.

[17] Observations showed that the 4th AEW (along longitude 23°W in the Figures 1 and 4) developed into Hurricane Helene over the Atlantic on Sep 13. Figure 4d shows the simulated track and best track. The initial location of Helene is predicted remarkably well on Day 22 with a displacement error of 300 km. The subsequent movement from Day 22 to Day 30 is quite realistic with the largest error of about 700 km on 19 Sep (Day 28). The intensity evolution is realistically simulated with a time lag of only 1–2 days (Figure 4e), indicating that the model not only simulates the rapid intensification stage from Sep. 15–18 but also the maintenance stage between from Sep. 18–21.

During the integration period, Hurricane Debby and Florence were also associated with specific AEWs. The control run realistically captured the movement of Debby but the formation of Florence had larger errors in timing and location, which are discussed in Figure S6. The exact reasons causing the larger error in Florence's formation are not a focus of this study. However, the differences in the location of where Florence and Helene formed may suggest the importance of improving oceanic feedbacks, which remains a hypothesis.

4. Concluding Remarks

[18] In this study, ten 30-day 0.25° simulations were conducted with the NASA global mesoscale model to understand the model's ability to simulate the initiation and propagation of 6 consecutive AEWs in late August 2006 and the mean state of the AEJ over both Africa and downstream in the tropical Atlantic with the aim of extending the lead time for the prediction of hurricane formation near the Cape Verde Islands.

[19] The control run initialized at 0000 UTC 22 August 2006 is discussed first. Over the 30-day period, 6 AEWs and the time-averaged AEJ are realistically simulated with the exception of the 5th and 6th AEWs, which had relatively larger errors in timing as compared to NCEP analysis and NAMMA observations. In addition, a mesoscale vortex appears after 22 days of integration and later develops into a hurricane. This simulated mesoscale vortex resembles the observed Hurricane Helene with respect to the genesis timing, location and initial intensity, and also to the subsequent movement and intensification.

[20] Previously, realistic simulations of hurricane climate statistics with numerical models and prescribed SSTs indicated the importance of accurately representing surface processes. With nine extended-range simulations, this study further confirms the importance of the accurate representation of initial land surface fields and their interactions with other fields. The finding are summarized as follows: (1) accurate representations of non-linear interactions between the atmosphere and land processes are crucial for improving the simulations of the consecutive initiation of AEWs and the AEJ, (2) that improved simulations of an individual AEW and its interaction with local environments (e.g., the Guinea Highlands) could provide determinism for hurricane formation downstream (e.g., Helene) and thus extend the lead time of formation prediction, (3) however, the dependence of AEW simulations on accurate dynamic and surface ICs and BCs poses a challenge in simulating their modulation on hurricane activity. Further analysis is still needed to examine the model's performance in simulating the conversion of energy among the AEJ, individual AEWs and meridional circulations.

[21] A recent trend in the study of tropical cyclogenesis processes is to examine the role of the critical layer/level (CL) associated with a tropical easterly wave [*Dunkerton et al.*, 2008]. The efficiency of energy absorption/reflection by the resolved CL in numerical models and other processes (e.g., wave accumulation) that lead to hurricane formation will be examined carefully in a further study.

[22] **Acknowledgments.** We would like to thank reviewers for their valuable suggestions, which have substantially improved the manuscript. We are grateful for the following organizations for supporting this study: NASA ESTO; AIST Program; MAP Program; NEWS and NSF STC. We would also like to thank Steve Lang for reviewing this manuscript and Karen More for helpful discussion. Acknowledgment is also made to the NASA HEC Program, the NASA NAS and NCCS for the computer time used in this research.

References

Atlas, R., et al. (2005), Hurricane forecasting with the high-resolution NASA finite volume general circulation model, *Geophys. Res. Lett.*, *32*, L03807, doi:10.1029/2004GL021513.

Berry, G. J., and C. Thorncroft (2005), Case study on an intense African easterly wave, Mon. *Weather Rev.*, *133*, 752–766, doi:10.1175/MWR2884.1.

Brown, D. P. (2006), *Tropical cyclone report: Hurricane Helene, Rep. AL082006*, Natl. Hurricane Cent., Miami, Fla.

Carlson, T. N. (1969), Synoptic histories of three Africa disturbances that developed into Atlantic hurricanes, *Mon. Weather Rev.*, *97*, 256–276, doi:10.1175/1520-0493(1969)097<0256:SHOTAD>2.3.CO;2.

Cornforth, R. J., B. J. Hoskins, and C. D. Thorncroft (2009), The impact of moist processes on the African easterly jet-African easterly wave system, *Q. J. R. Meteorol. Soc.*, *135*, 894–913, doi:10.1002/qj.414.

Dunkerton, T. J., M. T. Montgomery, and Z. Wang (2008), Tropical cyclogenesis in a tropical wave critical layer: Easterly waves, *Atmos. Chem. Phys. Discuss.*, *8*, 11,149–11,292, doi:10.5194/acpd-8-11149-2008.

Hall, N. M. J., et al. (2006), Three-dimensional structure and dynamics of African easterly waves. Part II: Dynamical modes, *J. Atmos. Sci.*, *63*, 2231–2245, doi:10.1175/JAS3742.1.

Hsieh, J.-S., and K. H. Cook (2005), Generation of African easterly wave disturbance: Relationship to the African easterly jet, *Mon. Weather Rev.*, *133*, 1311–1327, doi:10.1175/MWR2916.1.

Landsea, C. W. (1993), A climatology of intense (or major) Atlantic hurricanes, *Mon. Weather Rev.*, *121*, 1703–1713, doi:10.1175/1520-0493(1993)121<1703:ACOIMA>2.0.CO;2.

Lin, S.-J. (2004), A vertically Lagrangian finite-volume dynamical core for global models, *Mon. Weather Rev.*, *132*, 2293–2307, doi:10.1175/1520-0493(2004)132<2293:AVLFDC>2.0.CO;2.

Sander, N., and S. C. Jones (2008), Diagnostic measures for assessing numerical forecasts of African easterly waves, *Meteorol. Z.*, *17*, 209–220, doi:10.1127/0941-2948/2008/0269.

Schmidlin, F. J., B. Morrison, T. Baldwin, and E. T. Northam (2007), High resolution radiosonde measurements from Cape Verde: Details of easterly wave passage, *Eos Trans. AGU*, *88*(52), Fall Meet. Suppl., Abstract A21C-0641.

Shen, B.-W., R. Atlas, O. Reale, S.-J. Lin, J.-D. Chern, J. Chang, C. Henze, and J.-L. Li (2006), Hurricane forecasts with a global mesoscale-resolving model: Preliminary results with Hurricane Katrina (2005), *Geophys. Res. Lett.*, *33*, L13813, doi:10.1029/2006GL026143.

Shen, B.-W., W.-K. Tao, W. K. Lau, and R. Atlas (2010), Predicting tropical cyclogenesis with a global mesoscale model: Hierarchical multiscale interactions during the formation of tropical Cyclone Nargis (2008), *J. Geophys. Res.*, *115*, D14102, doi:10.1029/2009JD013140.

Thorncroft, C. D., and M. Blackburn (1999), Maintenance of the African easterly jet, *Q. J. R. Meteorol. Soc.*, *125*, 763–786.

Thorncroft, C. D., et al. (2008), Three-dimensional structure and dynamics of African easterly waves. Part III: Genesis, *J. Atmos. Sci.*, *65*, 3596–3607, doi:10.1175/2008JAS2575.1.

Wu, M.-L. C., et al. (2009), African easterly jet, structure and maintenance, *J. Clim.*, *22*, 4459–4480, doi:10.1175/2009JCLI2584.1.

Zipser, E. J., et al. (2009), The Saharan air layer and the fate of African easterly waves—NASA's AMMA field study of tropical cyclogenesis, *Bull. Am. Meteorol. Soc.*, *90*, 1137–1156, doi:10.1175/2009BAMS2728.1.

B.-W. Shen, W.-K. Tao, and M.-L. C. Wu, NASA Goddard Space Flight Center, Greenbelt, MD 20771, USA. (bo-wen.shen-1@nasa.gov)